Seismic analysis of earth, rockfill and concrete gravity dams

Michail S. Spyridis, Susana Lopez-Querol
University College London, London, United Kingdom

Pedro J. Martin-Moreta
Brunel University, London, United Kingdom

ABSTRACT: Failures of dam structures represent a catastrophic hazard, especially for the downstream populations, facilities and environment. Many failures of these structures have occurred in the past due to earthquakes, which emphasise the necessity of further research efforts in this line. The objective of this study is to evaluate the seismic vulnerability of dam structures pointing out the complexities and the consequences associated with such phenomena. A rigorous calculation of the seismic behaviour of earth, rockfill and concrete gravity dams is presented, with the aim to provide comprehensive numerical approaches. For this purpose, the water-dam-soil interaction effects are analysed in detail, with the focus to be on methods accounting for materials, geometrical and contact nonlinearities. Finally, the liquefaction susceptibility of earth dams is studied using a methodology based on the well-known semi-empirical relationships.

1 INTRODUCTION

In the past, failures have been occurred to dams not only due to earthquakes but also due to sloshing effects of the water and more commonly due to flooding. This phenomenon has the ability to induce significant damages in the dam body itself, but more importantly to the downstream populations and facilities. In Japan, Fujinuma earth dam resisted to the Tohuku ground shaking in 2011, but the water reservoir of 1.5 million cubic meters overtopped the dam due to the settlement of the crest approximately 20 minutes after the earthquake, inducing a catastrophic flood. The resultant of this flooding was, firstly, the collapse of the dam, and secondly-more importantly resulted in 8 casualties as well as in a destroyed village. Information about this event can be found in the literature [Abbas et al. (2011);Pradel et al. (2013)].

The earthquake fragility of dams can be identified in their failures during past events. One of the most well-known occurred in San Fernando earthquake, in 1971, with Mw 6.5, in which the upstream slope failed due to liquefaction, as Seed (1981) presented in his study, along with significant conclusions about the seismic performance of earthen dams. In contrast with earth dams, rockfill dams have the ability to resist moderate ground motions and in terms of drained conditions can stand strong ground shakings. Research innovations about their shear dynamic behaviour have been introduced in the literature [Ambraseys and Sarma (1967);Dakoulas and Gazetas (1985);Gazetas and Dakoulas (1992)]. Moreover, Koyna dam, in India, was a concrete gravity dam which experienced Koyna earthquake on December 1967 with Mw 6.5 and peak ground acceleration 0.49g, parallel to the plane section of the dam. The performance of the aforementioned dam was extensively been studied by Chopra and Chakrabarti (1973) who illustrated its damage levels, such as the horizontal cracking on both sides, and the relative displacements of the concrete monoliths due to their different elevations. The latter implies different fundamental periods between the monoliths which led them to oscillate in a different manner. The impact of this behaviour had as a resultant the failure of the vertical joints at the edges of the monoliths which increased the seepage.

Numerous studies have been published regarding the earthquake analysis of dams. An important role to this analysis played Westergaard (1933) who introduced the hydrodynamic forces of the reservoir system to the dam with equivalent masses. Later on, the finite fluid elements have been used to increase the accuracy, simulating the fluid-structure interaction effect with the

Eurelian approach [Chopra (1968);Hall and Chopra (1982); Fenves and Chopra (1984);] or with the Lagrangian approach [Wilson and Khalvati (1983);Bayraktar et al. (1994);Bilici et al. (2009)]. The "infinite" spaces of the reservoir and the foundation can be modelled as bounded domains with local and consistent boundaries [Lysmer and Kuhlemeyer (1969);Kellezi (2000);Kontoe et al. (2009)]. In this way, the dynamic stiffness matrices of the soil and fluid media tend to provide continuity to the system describing the behaviour of the infinite domain, in contrast with the elementary boundary conditions which completely reflect the propagating waves.

The motivation of this study comes from the seismic risk assessment of the major dams in the United States of America. In more detail, this paper presents the preliminary assessment of the seismic performance of three generic, typical types of dam in the U.S., i.e. earth, rockfill and concrete gravity dams. For the achievement of this objective, simplified numerical models have been developed, considering the foundation-dam-interaction effects. These models are used to illustrate the complete seismic behaviour of dams, with the focus to be on the identification of their most relevant potential failure modes.

2 FINITE ELEMENT MODELLING

In view of the achievement of the aforementioned objective, Finite Element Models are developed considering the water-dam-foundation interaction effects within ANSYS APDL. As said, the examined typologies of dams are earth dam, rockfill and concrete gravity dam (Fig.1). Earth dams are examined with two different shear wave velocities for its forming material, that is to say, 100 m/s and 250 m/s, preserving the rest of properties the same.

(a)

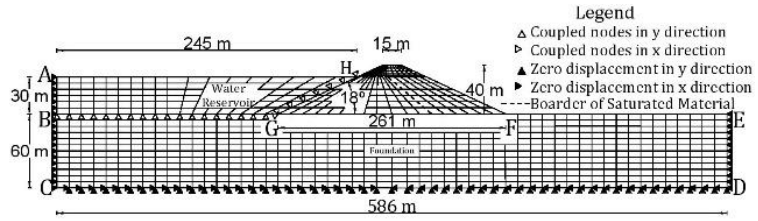

(b)

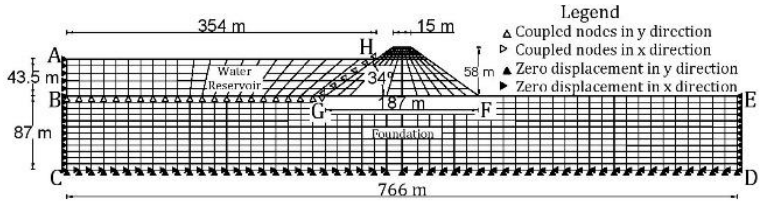

(c)

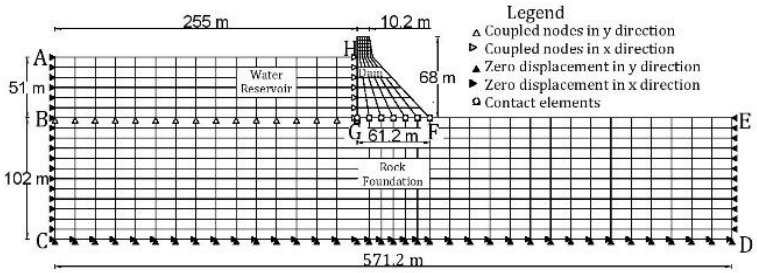

Figure 1 Finite element model geometry of a) earth dam b) rockfill dam c) concrete gravity dam

The numerical models are developed in the 2-dimensional space using the plane strain theory. They consist of two domains, the dam-foundation system with plane elements (Plane 182) and the reservoir system with fluid elements (Fluid 79). Emphasis has been given in the interfaces between these two systems, which are of great importance for the resultant dynamic behaviour of dams. For the reservoir interfaces with the dam and the foundation, the coupled method has been employed. In this way, the dynamic behaviour of the fluid is expressed in terms of dis-

placements Wilson and Khalvati (1983) and the sloshing effects are captured. Thus, the nodes of the reservoir with the corresponding ones of the foundation at their interface (BG in Fig.1) have the same vertical displacements, while the nodes of the reservoir are free to vibrate in the horizontal direction. On the other hand, in the dam-reservoir interface, the nodes have exactly the opposite restriction. It should be noted here that the nodes at the interface of the slope of the earthen dams have been rotated according to the angle of each type of them, as it can be noticed in Figure 1 (a & b) in interface GH. In the case of seismic excitation of concrete gravity dam, the grout curtain cannot ensure resistance against sliding Goldgruber et al. (2015). Therefore, the sliding is simulated with contact elements and the friction coefficient of the concrete interface with the rock foundation (GF) is considered equal to 0.65, as proposed in the aforementioned study. The described elements provide additional nonlinearities to the system.

The focus is on methodologies accounting for material and geometrical nonlinearities. Mohr-Coulomb and Drucker-Prager elasto-plastic laws have been adopted for soil and concrete, respectively. It should be noted that the complicated dynamic soil response cannot be captured by the former constitutive law, as it can describe mainly first-order models. This is mainly resulted in the stiffness and damping dependency on the strain level. Moreover, a homogeneous system for the dam body as well as for their foundations is assumed in all the models. In Table 1, the elasto-plastic properties for the materials in each type of dam can be found. According to previous case studies, concrete gravity dams are in general constructed of moderate strength concrete, due to low stresses, laying over firm foundations Office of Energy Projects (2016). For the geometrical parameters of this kind of dams, a typical plane section was selected as can be found in Chopra and Chakrabarti (1973).

On the other side, the geometrical properties of the earth and rockfill dam have been selected in such a way that they represent typical real dams in the U.S. Equal upstream and downstream slope angles have been adopted. For earth dams, Ambraseys and Sarma (1967) summarised important information on elastic properties, related to their height and age. From this study, two typical shear wave velocities are selected, representing not only different soil material (assumed homogeneous in this study), but also different compaction techniques. Finally, although the properties of a rockfill dam are known to be variable with the elevation, due to the confining pressure affecting the shear strength Gazetas and Dakoulas (1992), in this work, they have also been considered as homogeneous.

Table 1 Elasto-plastic properties of the materials in the modelled dams

Type of Dam		Elastic Properties			Mohr-Coulomb law				
		V_s(m/s)	ν	ρ(ton/m^3)	c(Pa)	φ(˚)	ψ(˚)	c´(Pa)	φ´(˚)
Earth	Soil	100 & 250	0.3	1.7 (2)*	$12\cdot10^3$	35	0	$6\cdot10^3$	25
	Foundation	650	0.3	2.1	$20\cdot10^3$	15	0	$15\cdot10^3$	10
Rockfill	Soil	720	0.3	2.1	$5\cdot10^3$	45	5	$2\cdot10^3$	35
	Foundation	1250	0.4	2.2	$15\cdot10^3$	30	0	$10\cdot10^3$	25
Gravity	Foundation	1500	0.45	2.2	$13\cdot10^6$	46	11.5	0	38
		Elastic Properties			Drucker-Prager law				
		E(MPa)	ν	ρ(ton/m^3)	R_c(MPa)	R_t(MPa)		R_b(MPa)	
	Concrete	$27.5\cdot10^3$	0.2	2.5	20	1.6		23	

*Mass of the saturated material; V_s: shear wave velocity; ρ: density; c: cohesion; φ: friction Angle; ψ: dilatancy angle; c´: residual cohesion; φ´: residual inner friction angle; E: Young's modulus; R_c: uniaxial compressive strength; R_t: uniaxial tensile strength; R_b: biaxial compressive strength

In addition to elementary boundary conditions, artificial boundaries have been implemented. In order to avoid permanent displacements with the commonly used absorbing boundaries Lysmer and Kuhlemeyer (1969), the cone boundary is employed, providing dynamic stiffness and viscous dashpots to the problem. Nevertheless, the stiffness of these artificial boundaries is a function of the distance from the source of excitation, the fault in case of earthquakes, which brings into light their drawback. The waves propagating through the fluid domain reflect at the dam, and thus it can be assumed that this is the source of excitation [Kontoe et al. (2009);Pelecanos et al. (2013)]. The same assumption has been considered for the foundation domain. Thus, the artificial boundaries are applied at the side abutment of the fluid (AB in Fig.1) in such a way that allows it to oscillate in the vertical direction. Stiffness-dashpots ele-

ments normally and tangentially oriented are at the nodes of the side abutments of the foundation (BC & DE). The nodes at the bottom of the latter (CD) have fully restricted displacements.

It should be noted that in the nonlinear transient analyses, the initial conditions due to the gravity loads are considered. In addition, Rayleigh damping is taken into account in the simulations, the parameters of which are determined by means of elastic behaviour considerations. It should be noted that the damping of the fluid elements is neglected in order to avoid unrealistic reductions in the hydrodynamic forces.

3 SEISMIC RESPONSE

The seismic performance of dams under 8 well-known ground motions has been investigated. Table 2 shows the selected ground motions and the estimation of the spectra acceleration for each type of dams based on their fundamental periods. Figure 2 illustrates their response spectra plotted for a range of fundamental periods of 2 sec. From this graph, it can be concluded that the most destructive earthquakes are Kobe and San Fernando due to the high spectral accelerations for a high range of fundamental periods, that is to say, to different types of structure.

Table 2 Ground motions and spectral acceleration

			Earth	Rockfill	Gravity
ID	Event	PGA*	$Sa(T_1)$, g	$Sa(T_1)$, g	$Sa(T_1)$, g
1	Imperial Valley	0.315	0.528	0.571	0.588
2	Kobe	0.821	1.486	1.762	1.797
3	Kocaeli	0.349	0.568	0.615	0.611
4	Nahanni	0.148	0.063	0.185	0.182
5	Northridge	0.217	0.186	0.481	0.488
6	Northridge 2	0.098	0.207	0.217	0.218
7	Parkfield	0.357	0.311	0.576	0.597
8	San Fernando	1.170	0.832	2.278	2.166

The results of the numerical models for all the dams are summarised in Table 3. For earth and rockfill dams, peak values of residual displacements in both directions, as well as in the relative horizontal accelerations at the crest of the dams, using both elementary and artificial boundary conditions, are jointly presented for comparison purposes. In the case of the concrete gravity dam, the results present the sliding at the base and horizontal displacements on top. As expected, Kobe and San Fernando earthquakes are the most destructive between all the examined ones. The former ground motion provided residual settlements of 0.83m (2.07% of the height of the dam) and 0.96m (1.65%) for earth and rockfill dams, respectively. In spite of the fact that these settlements reached up to approximately 2% of the height of the dams, no failures are predicted due to slide movements, especially in earth dams. In the case of the rockfill dam, concentrated strains are observed at the downstream slope, indicating some slope instability, without reaching failure though (Figure 3). Nevertheless, in this range of residual displacement, there is the potential of flooding or seepage due to the reduced freeboard, cracks in the main body or damages in the secondary elements, such as in the concrete face slab.

For the concrete dams, Tekie and Ellingwood (2003) stated that sliding greater than 0.15m could affect the ability of the dam to retain water. Between the examined ground motions, 4 out of 8 exceeded this threshold, i.e. Imperial Valley, Kobe, Kocaeli and San Fernando. Kobe earthquake resulted in greater sliding than for San Fernando earthquake, while in terms of relative horizontal displacements at the concrete domain display the opposite behaviour. Therefore, for San Fernando shaking, the main body dissipates energy to a great extent, whereas for Kobe earthquake the energy is mainly dissipated in the dam-foundation interface. This illustrates the importance of dam-foundation-reservoir interaction in the nonlinear solution. Finally, in Table 3, it can be observed that the three examined types of dam can resist moderated intensity ground shakings in terms of displacements. For instance, no significant movements have been obtained from the inputted ground motion of Parkfield, which has a peak ground acceleration of 0.357g.

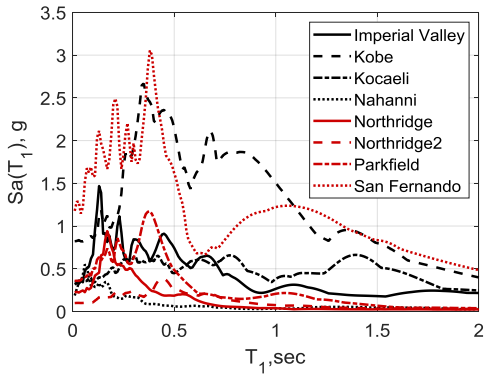

Figure 2 Response spectra

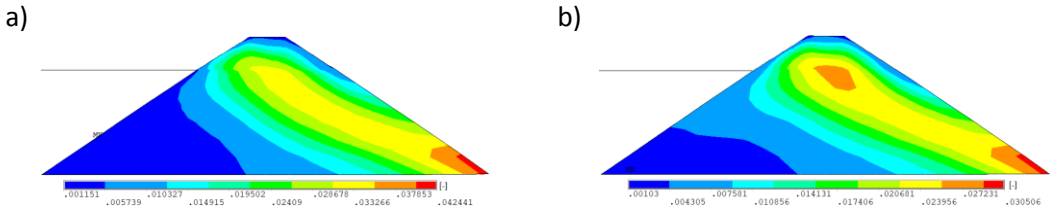

Figure 3 Von Misses strains in rockfill dam body: a) Kobe earthquake b) San Fernando earthquake

The importance of artificial boundary conditions is also presented in Table 3. In the case of the earthen dams, the difference is of minor importance in general, with the maximum to be at the horizontal displacements and accelerations, 10.2% and 11.9%, both for rockfill dams. However, the same cannot be stated for the reduced finite domain of concrete gravity dams, for which the error exceeded 30% in two cases. This difference can lead engineers to wrong assessment or design considerations. For this reason, the artificial boundary conditions become of great importance in critical projects, and thus, they should be used for these dams.

Table 3 Seismic performance at the crest of earth and rockfill dams with elementary boundary conditions and percentage difference with numerical models with cone boundary conditions

	Hor. Displacement at Crest, m		Settlement at Crest, m		*Hor. Acceleration at Crest, g		Sliding, m	**Rel. Displ. ,m
ID	Earth	Rockfill	Earth	Rockfill	Earth	Rockfill	Concrete Gravity	
1	0.16 (0.64)	0.32 (0.63)	0.24 (0.41)	0.22 (4.22)	0.79 (0.89)	0.81 (2.68)	0.29 (28.9)	0.05 (31.3)
2	0.85 (0.82)	1.45 (2.66)	0.83 (0.60)	0.96 (0.21)	1.08 (0.09)	1.16 (2.35)	0.95 (1.77)	0.11 (8.14)
3	0.26 (0.39)	0.34 (3.26)	0.31 (0.65)	0.19 (3.19)	0.57 (4.64)	0.85 (11.9)	0.18 (22.8)	0.03 (9.23)
4	0.01 (0.00)	0.02 (6.45)	0.06 (0.00)	0.02 (0.00)	0.26 (3.14)	0.47 (8.02)	0.01 (15.4)	0.02 (6.90)
5	0.03 (3.17)	0.04 (2.35)	0.06 (1.68)	0.05 (2.25)	0.46 (3.08)	0.73 (6.09)	0.05 (33.8)	0.03 (6.90)
6	0.03 (3.08)	0.03 (10.2)	0.07 (5.97)	0.03 (6.45)	0.42 (0.47)	0.41 (6.48)	0.01 (0.00)	0.02 (10.5)
7	0.06 (1.74)	0.17 (5.59)	0.12 (1.71)	0.15 (0.00)	0.90 (0.67)	0.81 (3.01)	0.12 (14.6)	0.05 (12.2)
8	0.46 (1.10)	0.65 (5.96)	0.71 (0.28)	0.78 (1.43)	1.20 (0.33)	1.16 (12.9)	0.55 (10.9)	0.25 (32.2)

*Relative acceleration at the crest of the dam; **Relative horizontal displacement between the top-base of dam; In brackets, the percentage difference with cone boundary conditions, %;

The seismic behaviour of both earth dams and rockfill dam is analysed in detail in Figure 4, where the vertical profiles of peak horizontal displacement and total acceleration, as well as the response spectra at the crest of the dams, are given. Looking, initially, at the peak horizontal displacements of the foundations, it can be observed that they increase almost monotonically with height. In more detail, the comparison between the two earth dams (with V_s 100 and 250 m/s) is of particular interest, pointing out the importance of dam-foundation interaction: the earth dam with higher shear modulus imposes its foundation to be of greater deformability, due to its ability to better resist in the ground shaking, in contrast with the more flexible dam. In the latter case, higher residual deformations are generally observed in the body of the dam. However, this does not imply that the deformation at the crest of the dam is only a function of the shear modulus, but also of the geometrical features such as the height and the slope angle. That finding is confirmed by the high deformations in the stiff rockfill dam.

In all of the examined dams, the peak horizontal displacements produced by the Kobe earthquake are greater than in the rest of the inputted ground motions. On the other hand, San Fernando earthquake provides higher total accelerations in the dam-foundation systems. In these strong shakings, the foundation of the dams absorbs a significant amount of energy, which results in smaller peak ground accelerations. In addition, the response spectra at the top of the dams illustrate that the ground motions can be significantly amplified, especially for a stiff dam. On the other hand, the flexibility of earth dams with shear wave velocity 100 m/s, provides higher spectra accelerations to a great range of fundamental periods.

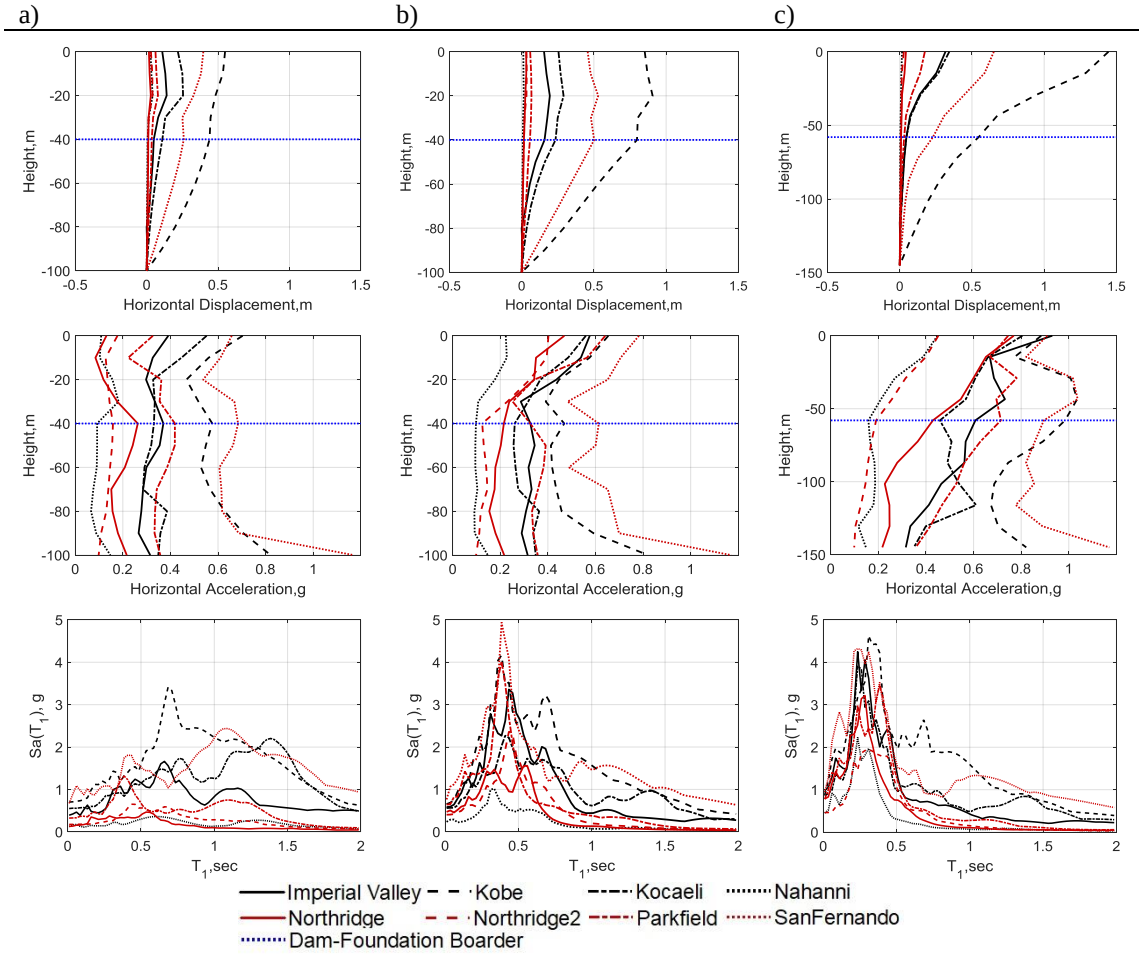

Figure 4 Vertical profile of peak displacement, peak horizontal total acceleration and response spectra (ζ=5%): a) earth dam Vs 100 m/s b) earth dam Vs 250 m/s c) rockfill Dam

Looking past failures of earth dams, it has been observed that a significant number of them suffered from liquefaction, leading to sliding movements and loss of elevation. This failure is related to the development of the excess pore-water pressure during earthquakes in soils with

small proportion of low plasticity fines. In such conditions, the solid-state principals of the soil are not applied, and instead it behaves like a liquid.

In this study, the semi-empirical relationship by Youd et al. (2001) is combined with the Finite Element solution for the susceptibility of liquefaction in earth dams. Hence, the improvement of this work brings into light a rigorous calculation of the total and shear stresses (and thus, the Cyclic Shear Ratio – CSR) in the dam at different locations nearby the upstream slope, and thus a better estimation of the effective stresses. Nevertheless, the described calculation of CSR does not necessitate a comprehensive method for potential liquefaction, therefore it must only be used by specialised experts and only in noncritical projects.

Dynamic shear stresses trigger liquefaction, as the evolution of volumetric strains results in the increase of pore water pressure, and thus the effective stresses of the solid skeleton tend to zero. Therefore, in this research the history of CSR is obtained as the difference between maximum shear stresses due to gravity loads, $\tau_{max,st}$, and those induced by dynamic loads, $\tau_{max,dyn}$. Finally, the cyclic resistance ratio (CRR) is estimated from Roberston's et al. curve Youd et al. (2001), which is corrected by the magnitude correction factor, MSF, and the correction of confining stress, K_σ. According to this methodology, the earth dam with shear wave velocity 250 m/s is not susceptible to liquefaction.

For the aforementioned reason, the Safety Index (S.I.), as defined in Eq.1, is initially equal to zero in the time-histories of the examined locations at the upstream slope of the dam, Figure 5. Figure 5 shows that, where the S.I. exceeds the threshold (from above or below 1), the likelihood of liquefaction is high. Consequently, the percentage of exceedance in each case is determined and presented in each graph of the figure, which can be considered of a measurement of the potential of liquefaction throughout a whole event for each location.

$$\text{S.I.} = \frac{\text{CSR}}{\text{CRR}_{7.5} \cdot \text{MSF} \cdot K_\sigma} = \frac{\frac{\tau_{max,st} - \tau_{max,dyn}}{\sigma_o'}}{\text{CRR}_{7.5} \cdot \text{MSF} \cdot K_\sigma} \quad (1)$$

In the case of Kobe and San Fernando earthquakes, the exceedance percentage is high indicating great liquefaction potential. Nevertheless, the time-histories of S.I. brought to the fore the question if liquefaction could be likely in cases such as the Northridge earthquake for the analysed dam, as it only exceeds the threshold slightly. Moreover, S.I. oscillations around non-zero values indicate residual maximum shear stresses induced by the yielding of soil and local pressures due to the upstream reservoir.

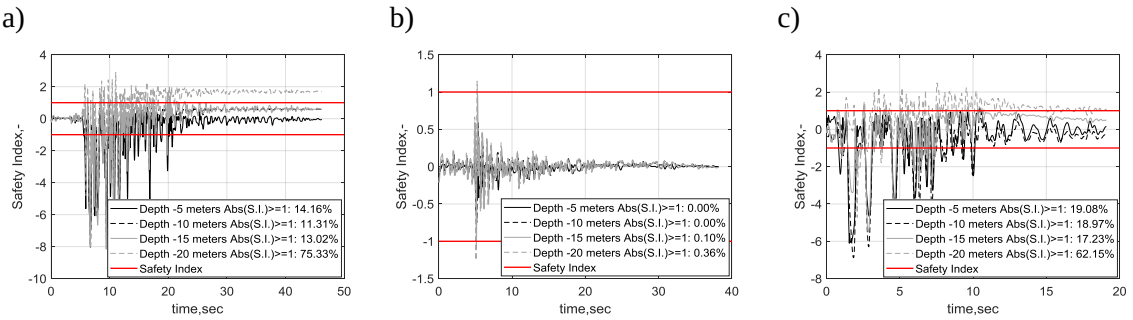

Figure 5 Time-history of liquefaction safety index: a) Kobe b) Northridge c) San Fernando

4 CONCLUSIONS

The seismic behaviour of three types of dam is examined in this study. Emphasis has been given to the interfaces of the dam-foundation-reservoir systems, methods accounting for nonlinearities and in dynamic simulation of the unbounded soil and fluid media.

The dynamic performance of concrete gravity dam resulted in great sliding displacements during strong shakings which can lead in loss of the control of the water reservoir or to seepage. In addition, the nonlinear complex behaviour of the dam-foundation-reservoir interaction has il-

lustrated that a concrete gravity dam can dissipate energy not only through the concrete domain but also from the dam-foundation interface.

On the other side, no significant sliding has been derived from the earth dams, although in the rockfill dam concentrated stains are observed in the downstream slope, which is mainly induced by its steep angle. This implies that the stiff rock material has the ability to resist even to strong shakings. However, the amplitude of residual displacements in strong shakings can lead to damages of the secondary elements (like upstream slabs) and in unfavourable conditions, such as in cases of a full reservoir, to flooding due to the reduced freeboard. In addition, the comparison of the earth dams has brought into light the significance of their dam-foundation interaction. Higher deformations can be observed in foundations which support relative stiff earth dam in contrast with a foundation which supports a flexible earth dam.

Finally, earth dams suffer from liquefaction susceptibility. In this study, the semi-empirical relationship by Youd et al. (2001) have been employed for this, with the improvement to be at the estimation of the Cyclic Shear Ratio. This analysis confirmed the potential liquefaction in earth dams for some of the analysed input loadings, without providing significant information regarding the triggering of liquefaction. For this reason, further research is needed in the simplified procedures of liquefaction.

REFERENCES

1. Abbas, M., Shiro, T., Sepand, S., 2011. Fujinuma dam performance during 2011 Tohoku earthquake , Japan and failure mechanism by FEM, in: 15 WCEE.
2. Ambraseys, N.N., Sarma, S.K., 1967. The response of earth dams to strong earthquakes. Géotechnique 17, 181–213.
3. Bayraktar, A., Dumanoğlu, A.A., Calayir, Y., 1994. Asynchronous dynamic analysis of dam-reservoir-foundation systems by the Lagrangian approach. Computers and Structures 58, 925–935.
4. Bilici, Y., Bayraktar, A., Soyluk, K., Haciefendioğlu, K., Ateş, Ş., Adanur, S., 2009. Stochastic dynamic response of dam-reservoir-foundation systems to spatially varying earthquake ground motions. Soil Dynamics and Earthquake Engineering 29, 444–458.
5. Chopra, A.K., 1968. Earthquake behavior of reservoir-dam systems. Journal of the Engineering Mechanics Division 94, 1475–1500.
6. Chopra, A.K., Chakrabarti, P., 1973. The Koyna earthquake and the damage to Koyna dam. Bulletin of the Seismological Society of America 63, 381–397.
7. Dakoulas, P., Gazetas, G., 1985. A class of inhomogeneous shear models for seismic response of dams and embankments. International Journal of Soil Dynamics and Earthquake Engineering 4, 166–182.
8. Fenves, G., Chopra, A.K., 1984. Earthquake analysis of concrete gravity dams including reservoir bottom absorption and dam-water-foundation rock interaction. Earthquake Engineering & Structural Dynamics 12, 663–680.
9. Gazetas, G., Dakoulas, P., 1992. Seismic analysis and design of rockfill dams: state-of-the-art. Soil Dynamics and Earthquake Engineering 11, 27–61.
10. Goldgruber, M., Shahriari, S., Zenz, G., 2015. Dynamic sliding analysis of a gravity dam with fluid-structure-foundation interaction using finite elements and Newmark's sliding block analysis. Rock Mechanics and Rock Engineering 48, 2405–2419.
11. Hall, J.F., Chopra, A.K., 1982. Two-dimensional dynamic analysis of concrete gravity and embankment dams including hydrodynamic effects. Earthquake Engineering & Structural Dynamics 10, 305–332.
12. Kellezi, L., 2000. Local transmitting boundaries for transient elastic analysis. Soil Dynamics and Earthquake Engineering 19, 533–547.
13. Kontoe, S., Zdravkovic, L., Potts, D.M., 2009. An assessment of the domain reduction method as an advanced boundary condition and some pitfalls in the use of conventional absorbing boundaries. International Journal for Numerical and Analytical Methods in Geomechanics 33, 309–330.
14. Lysmer, J., Kuhlemeyer, R.L., 1969. Finite dynamic model for infinite media. Journal of the Engineering Mechanics Division 95, 859–878.
15. Office of Energy Projects, 2016. Engineering guidelines for the evaluation of hydropower projects in: Gravity Dams.

16. Pelecanos, L., Kontoe, S., Zdravković, L., 2013. Numerical modelling of hydrodynamic pressures on dams. Computers and Geotechnics 53, 68–82.
17. Pradel, D., Wartman, J., Tiwari, B., 2013. Failure of the Fujinuma dams during the 2011 Tohoku earthquake. Geo-Congress 2013: Stability and Performance of Slopes and Embankments III 1559–1573.
18. Seed, H.B., 1981. Earthquake-resistant design of earth dams. Canadian Geotechnical Journal 4, 1–27.
19. Tekie, P.B., Ellingwood, B.R., 2003. Seismic fragility assessment of concrete gravity dams. Earthquake Engineering and Structural Dynamics 32, 2221–2240.
20. Westergaard, H.M., 1933. Water pressures on dams during earthquakes. Transactions of the American Society of Civil Engineers 98, 418–433.
21. Wilson, E.L., Khalvati, M., 1983. Finite elements for the dynamic analysis of fluid-solid systems. International Journal for Numerical Methods in Engineering 19, 1657–1668.
22. Youd, B.T.L., Idriss, I.M., Andrus, R.D., Arango, I., Castro, G., Christian, J.T., Dobry, R., Finn, W.D.L., Jr, L.F.H., Hynes, M.E., Ishihara, K., Koester, J.P., Liao, S.S.C., Iii, W.F.M., Martin, G.R., Mitchell, J.K., Moriwaki, Y., Power, M.S., Robertson, P.K., Seed, R.B., Ii, K.H.S., 2001. Liquefaction resistance of soils: Summary report from the 1996 NCEER AND 1998 NCEER / NSF workshops on evaluation of liquefaction resistance of soils 127, 817–833.